15 Sep 2022

Long-Time Kinetic Impact on Key Factors Affecting Asphaltene Precipitation

Ato Kwamena Quainoo

Abdulmohsin Imqam
Missouri University of Science and Technology, ahikx7@mst.edu

Recommended Citation

A. K. Quainoo and A. Imqam, "Long-Time Kinetic Impact on Key Factors Affecting Asphaltene Precipitation," *Energy and Fuels*, vol. 36, no. 18, pp. 11108 - 11122, American Chemical Society, Sep 2022. The definitive version is available at https://doi.org/10.1021/acs.energyfuels.2c01963

energy&fuels

pubs.acs.org/EF

Article

Long-Time Kinetic Impact on Key Factors Affecting Asphaltene Precipitation

Ato Kwamena Quainoo and Abdulmohsin Imqam*

Cite This: *Energy Fuels* 2022, 36, 11108−11122

Read Online

ACCESS | Metrics & More | Article Recommendations | Supporting Information

ABSTRACT: The employment of predictive techniques combining kinetic and thermodynamic analyses is the succinct solution to effectively control asphaltene precipitation during crude oil production. Although thermodynamic processes and conditions have been well studied in the literature, the effect of long-time kinetics on the key factors affecting the precipitation of asphaltenes was not critically studied. This work employed a model oil for asphaltene precipitation long-time kinetic observations. Filtration and confocal microscopy experimentations for time periods of 0−7200 min were utilized to study asphaltene yields and sizes at room and high temperatures (25, 50, and 70 °C), rotation speeds (60 and 150 rpm), and precipitant concentrations (50 and 60 wt %). The results from both experiments were fitted with DLVO models. The experimental results confirmed that the effects of temperature, rotation speeds, and precipitant compositions on asphaltene precipitation were significantly affected by time. The asphaltene yields increased from 27 to 83% within 7200 min when the heptane concentration increased from 50 to 60 wt %. Conversely, increasing temperatures from 25 to 70 °C reduced the cumulative asphaltene yields by 20−40% when observed for a long time (0−7200 min). Significant reductions in the mean equivalent diameter (MED) of precipitating asphaltenes upon increasing temperature within the studied timeframes were observed via the confocal experimentations. The rotation speeds also showed an inverse relationship with asphaltene yields and particle size. A reduction from 30 to 50% of the yield was observed as the rotation speeds of the system were increased from 60 and 150 rpm. The results of this work confirmed the significant impact of contact time on the precipitation of asphaltenes. In addition, DLVO theory employed to predict the experimental data obtained from the confocal microscopy fitted the data with mean absolute errors ranging from 4.44 to 5.15, which showed significant limitations upon increasing temperature. This development is progress toward enhancing the predictability of a production route devoid of asphaltene-related problems.

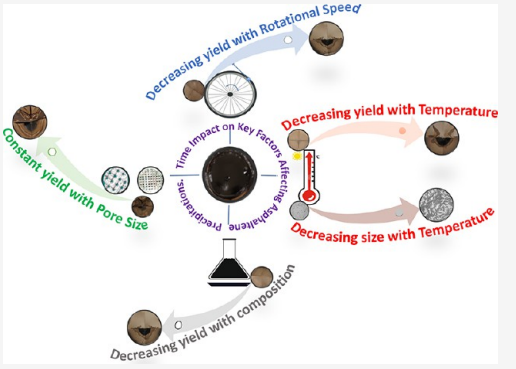

1. INTRODUCTION

The application of enhanced oil recovery (EOR) processes such as miscible gas flooding proved to improve oil recovery from reservoirs challenged with pressure depletion.[1−4] The intrusion of the gas composition during EOR destabilizes the asphaltene content of the crude resulting in the precipitation of asphaltenes.[5,6] Although the initial particle size of precipitating asphaltenes lies within the diametric size of nanometers to microns, their abilities to flocculate and aggregate into large-diameter particles (to several hundreds of microns, >100 μm) is the real challenge in the industry.[7,8] These large particles with adsorption affinity for solid surfaces cause flow assurance problems such as clogging of production facilities, wells, pipelines, and subsurface formations.[9−11] Creek et al.[12] highlighted that over 1.2 million dollars are lost per day due to asphaltene precipitation-related problems. Previous studies aimed at resolving asphaltene precipitation during oil production highlight that asphaltene precipitation is strongly influenced by the varying thermodynamic nature of the medium in which they are contained.[13] Temperature, pressure, fluid composition, and particle concentration are the common thermodynamic parameters known to strongly influence asphaltene precipitation.[14]

The effects of these thermodynamic parameters on the precipitation of asphaltenes were proven to be time-dependent. However, the extent to which time impacted the precipitation ability of these parameters was often neglected in the literature. Most studies investigating asphaltene precipitation by thermodynamic parameters were conducted under short-time scales ranging from 1 to 2880 min.[15,16] Recent studies over the past two decades hinted at the over-prediction of asphaltene precipitation by several short-time kinetic experimentations.[17] Beck et al.[18] indicated that asphaltene yields would gradually increase as long as the medium is observed. The lack of long-

Received: June 13, 2022
Revised: August 19, 2022
Published: August 31, 2022

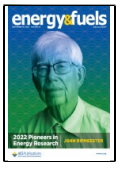

time asphaltene precipitation experimentations highlighted a significant area for research to holistically understand the mechanisms of asphaltene precipitation. An accurate study will lead to the generation of precise thermodynamic models with a high degree of certainty in predicting asphaltene precipitation.

Maqbool et al.[15] initiated the study of long-time effects on the precipitation of asphaltenes via centrifugation experimentation. Their study confirmed the continuous precipitation of asphaltenes from several days to even months before reaching their thermodynamic limit. Maqbool et al.[19] also investigated the effect of temperature (25−50 °C) for a long time (0−52 h) and observed the continuous precipitation of asphaltenes. They observed that temperature significantly influenced asphaltene precipitation by improving its solubility in its medium. Increasing solubility therefore led to less precipitation of asphaltenes. By contrast, Ghanavati et al.[20] stated that increasing temperature increases the solubility of the resins and reduced the viscosity of the oil system. These then lead to an increase in asphaltene precipitation and aggregation. For clarity, long-time kinetic studies investigating the effect of increasing temperature under mimicked reservoir conditions on asphaltene precipitation are needed. Furthermore, Maqbool et al.[19] employed a direct centrifugation method to determine the amount of precipitating asphaltenes for their entire studied time. This method was challenged by several complexities such as numerous heptane washings of the filter cake on the walls of the centrifuge tube and the application of a temperature evaporation process. This method could be difficult to replicate. To address the complexities regarding the direct centrifugation technique, authors proposed indirect methods such as magnetic resonance imaging, focused beam reflectance measurements, ultraviolet−visible spectroscopy, and near-infrared (NIR) region.[21] However, the indirectness of these methodologies were not sufficiently validated to accurately mimic asphaltene precipitation yields and sizes.[22] Studies of asphaltene precipitation with simple and direct techniques under long-time experimentations are needed to address the complex issues with high validations. Rogel and Moir[23] employed a direct filtration technique to study the effect of time and solvency power on asphaltene yields. Although they employed a suitable direct experimentation, the impact of temperature, rotation speed (agitation of the system), and composition on asphaltene yield and particle size under long time scales were not investigated. The effect of long time on the factors that influenced the precipitation of asphaltenes during oil production is lacking in the literature.

This paper employed the direct filtration technique and confocal microscopy to study the effects of varying fluid composition, temperature, and rotation speed (agitation) on asphaltene precipitations in a model oil system observed under room and in situ conditions. The employment of a model oil comprising only asphaltenes, toluene (solvent), and heptane (precipitant) mimicked a system with reduced complexities. This system enabled a better understanding of asphaltene precipitation in the absence of many unknowns present in a given crude oil system.[24] Also, the obtained experimental data were evaluated for prediction with the DLVO models. These models proved to predict kinetic data with accuracy. The outcome of this work built capacity for the holistic study of asphaltene precipitation under in situ conditions, and it aided in designing a suitable predicting system profitable for petroleum production projects.

2. MATERIALS AND METHODOLOGY

2.1. Materials Used in This Study. This study focused on kinetics experimentation via a direct filtration technique using a model oil system comprising asphaltenes, toluene, and heptane. The model oil system employed provided a system with reduced interactional effects between the other constituents of the crude (saturates, aromatics, and resins) and the asphaltenes. Furthermore, the model oil system gave a transparent and less viscous fluid composition for confocal microscopy studies. The model system was proven to be Newtonian, thus fitting for representing crude.[25]

First, the unwashed asphaltenes utilized for the experimentation were extracted from a Western Missouri asphaltenic crude oil with an asphaltene content of 13.5 wt %. Herein we employed a modified IP 143 method for the extraction. Although the ASTM D6560 method is considered the standard test method for the determination of asphaltenes (Heptane Insolubles) in Crude Petroleum and Petroleum Products, the modified method employed in this study has been also considered as a fast and reliable method of preparing asphaltenes in the laboratory. This method followed the industry standard procedure used to test for saturates, aromatics, resins, and asphaltenes (SARA).[4,26]

This extraction was done by adding 40 mL of *n*-heptane precipitant to a gram of the crude in a conical flask following the experimental procedure described elsewhere.[26,27] The crude oil−heptane mixture was stirred for 1440 min with a magnetic stirrer after which the resultant solution was filtered with a 2.7 μm pore size filter paper (Whatman's No. 2) using closed chamber filtration apparatus (see Figure 1a) for another 1440 min. To prevent heptane evaporation, the beaker was capped from the top. The agitated sample was placed into the filter apparatus, which was then sealed at the top. After 1440 min, the sample was filtered. The obtained filter cake known as the wet precipitated asphaltenes (see Figure 1b) was dried to obtain the dry unwashed asphaltenic particles (see Figure 1c). Toluene was used as the solvent for asphaltenes, n-heptane was used to initiate the precipitation of the asphaltenes as precipitants, and lastly, *n*-hexane was used as the precipitant for the GC−MS crude oil characterization.[28] The following calculation was done to obtain asphaltene weight percent:

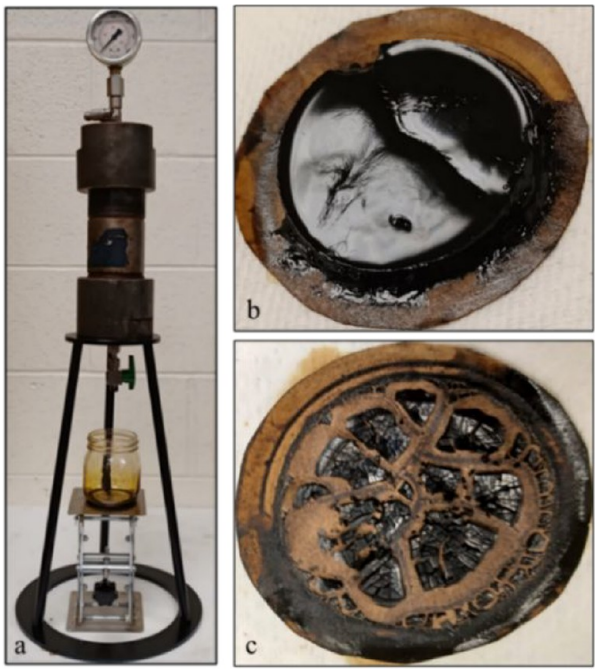

Figure 1. (a) Filtration apparatus used for asphaltene extraction; (b) wet precipitated asphaltene; (c) dry precipitated asphaltenes.

https://doi.org/10.1021/acs.energyfuels.2c01963
Energy Fuels 2022, 36, 11108−11122

$$\text{asphaltene weight percent} = \frac{w_{af} - w_{bf}}{A_t}$$

where w_{bf} is the weight of filter paper before filtration, w_{af} is the weight of filter paper after filtration, and A_t is the total amount of asphaltene dissolved in a sample.

All weighing was performed using the Ohaus EX324N/AD Explorer Analytical High Precision Scale Balance with readability and repeatability of 0.001 g. The molecular weights and percentage purity of the chemicals, including the supplier of the chemicals used in this study, are summarized in Table 1. All the chemicals were used without further processing or purification.

Table 1. List of Properties and Suppliers of the Chemicals/Materials Utilized in This Study

chemical	chemical formula	M_W (g/mol)	purity	supplier
heptane	C_7H_{16}	100.21	≥99%	Lab Alley Powering Science
toluene	C_7H_8	92.14	≥99%	Fisher Scientific
hexane	C_6H_{14}	86.18	≥99%	Lab Alley Powering Science
crude oil				Western Missouri Oil Field
Whatman 2.7 μm filter paper				OFITE, Inc. Filter paper

The light and heavy components of the crude oil utilized for the asphaltene extraction were also determined using the GC−MS with the 7683B Liquid Autosampler by Agilent Technologies. Before the start of each experimental run, 0.5 μL of a 0.05% dilute crude oil solution (in hexane) was loaded into the instrument under the following conditions: helium (carrier gas at 0.8 mL/min); temperature (40−325 °C), and injection volume (2.0 μL), The injection port was split at 250 °C and the system capillary column is 30 m × 0.25 mm i.d. × 0.25 μm film thickness. The detector was maintained at 230 °C. The oven was maintained at 60 °C for 2 min, and then the temperature was increased to 250 °C (10 °C/min); this temperature was maintained for 20 min. All the peaks were identified from their mass spectra by comparison with spectra in Wiley6N and NIST98 libraries utilizing their retention times and area %.[29] The composition of the crude is summarized in Table 2.

Table 2. Composition of the Asphaltene-Free Maltene Fraction of the Crude Oil

composition	mass %	composition	mass %
C_4	4.90	C_{14}	11.61
C_5	1.60	C_{16}	17.05
C_6	2.97	C_{17}	2.29
C_7	3.61	C_{18}	10.27
C_8	10.49	C_{20}	12.65
C_9	0.46	C_{22}	4.60
C_{10}	1.68	C_{27}	0.76
C_{11}	1.90	C_{29}	1.25
C_{12}	2.21	total	100%
C_{13}	0.92		

2.2. Asphaltene Yield vs Time Measurements Using Filtration Experiments. In this study, a direct filtration technique was employed to measure the amount of aggregating asphaltenes at varying times. First, 5 wt % asphaltenes were dissolved in toluene and sonicated for 60 min to ensure a homogeneous mixture. We do understand that asphaltene contents in typical light oil reservoirs are <4.56 wt %; however, the aim of this work was to investigate the kinetics of asphaltene precipitation under harsh experimental conditions of moderate-high asphaltene contents (using 5 wt % asphaltenes) before simulating actual field conditions. This will provide the understanding of asphaltene precipitations in actual visible systems. After the mixture of toluene and asphaltenes was made, a known volume of heptane was added to the asphaltene−toluene mixture gradually; the mixture was steady-shirred intermittently to achieve a homogeneous mixture. The selection of the heptane concentration ratio was largely dependent on the concentration of the solvent used (toluene). Research studies suggest that the onset of asphaltene precipitation in model oil systems is stimulated at concentrations of the precipitant equal to and above the solvent concentration (50%).[26] This work employed two systems. The first contained heptane at thermodynamic equilibrium (heptane:toluene concentration of 50:50%), and the other contained heptane concentrations above the solvent concentration (heptane:toluene concentration of 60:40%). The latter system is more likely to stimulate the flocculation of asphaltene particles needed for precipitation studies.

Next, the precipitation of the asphaltenes in the homogeneous mixture of heptane, toluene, and asphaltenes were evaluated for the entire studied time upon varying conditions of rotation speed, filter papers, and temperature. The varying rotation speeds accounted for the effects of extremely low and high pipeline shear during production.[30] Varying temperatures monitored the effects of room and high temperatures on the precipitation of asphaltenes, respectively, and the varying filter papers monitored the effects of reservoir pores on asphaltene precipitation. The asphaltene yield measurements were obtained via timely carried out filtrations using the Whatman 42 filter papers. The various conditions for the asphaltene yield versus time experiments are summarized in Table 3.

Table 3. Studied Systems and Conditions for Asphaltene Yield Versus Time Experimentations

heptane:toluene concentration	temperature	asphaltene content	shear rate	paper size
Effect of heptane concentration				
60:40 (system A)	25 °C	5 wt %	60 rpm	2.7 μm
50:50 (system B)	25 °C	5 wt %	60 rpm	2.7 μm
Effect of shear rate				
60:40	25 °C	5 wt %	60 rpm	2.7 μm
60:40	25 °C	5 wt %	150 rpm	2.7 μm
Effect of temperature				
60:40	25 °C	5 wt %	60 rpm	2.7 μm
60:40	50 °C	5 wt %	60 rpm	2.7 μm
60:40	70 °C	5 wt %	60 rpm	2.7 μm
Effect of filter paper size				
60:40	25 °C	5 wt %	60 rpm	2.7 μm
60:40	25 °C	5 wt %	60 rpm	0.45 μm

The volume of heptane added to the asphaltene-toluene mixture and the conditions under which the model oil systems were prepared are summarized in Table 4.

2.3. Particle Size Analysis Using Confocal Microscopy. The size distributions of precipitating asphaltenes under conditions of low shearing, varying temperature, and precipitant compositions were evaluated using a super-resolution imaging ECLIPSE Ti2 inverted laser scanning confocal microscope. Confocal microscopy provided clear particle size images from a thin section of a thick sample. The obtained microscopy images were analyzed with Nikon's powerful acquisition and analysis software, NIS-Elements. In this study, a heptol (heptane and toluene) mixture with an asphaltene content of 5 wt % and a heptane:toluene ratio of 1.5 was used for the particle size analysis. Thin sections were analyzed under the microscope for different time intervals (0−7200 min). The obtained microscopic images were further processed and analyzed with the advanced threshold technique from the MIPAR Image Processing tool. Utilizing

https://doi.org/10.1021/acs.energyfuels.2c01963
Energy Fuels 2022, 36, 11108−11122

Table 4. Conditions under Which the Yield and Particle Size Analysis Were Conducted

experimentation	system A (60% heptane)	system B (50% heptane)
heptane concentration	**60%**	**50%**
toluene concentration	40%	50%
filtration time	180 min	180 min
drying time	180 min	180 min
paper size	2.7 μm	2.7 μm
temperature	25−70 °C	25 °C
pressure	14.7 psi	14.7 psi
volume of filtrate	1−1.5 mL	1.5 mL
stirrer's rotation speed	60 and 150 rpm	60 rpm
studied time	7200−30,090 min	7200 min
total diluted asphaltenes	5 wt %	5 wt %

the processing tool, the mean equivalent diameter and particle counts were determined for each microscopic image.

2.4. DLVO Modeling of Asphaltene Cluster-Cluster Precipitations. In this study, the classical Derjaguin−Ladau−Verwey−Overbeek (DLVO) theory was employed to predict the colloidal structural evolution of the precipitating asphaltene particles. The term classical implied that only the attractive and repulsive interactions involving asphaltene precipitation were considered. The main assumptions for this theory included the following: (a) asphaltenes are solid particles suspending as colloids in the crude oil stabilized by resin, and (b) the asphaltene precipitation process is a thermodynamic irreversible process.

Two models of the DLVO theory [diffusion-limited aggregation (DLA) model and reaction-limited aggregation (RLA) model] were employed to fit the time-particle size measurements. The DLA model was employed when two particles aggregating in solution stuck to one another upon collision. DLA, therefore, occurred when the colloids' surface repulsive charges were low. The asphaltene particle size was described by fast-aggregation kinetics and is described with eq 1, as follows:

$$R = R_o\left[1 + \frac{t}{\tau_D}\right]^{1/d_f} \quad (1)$$

where R is the radius of aggregates at any time t; R_0 is the initial radius of the particles; d_f is the fractal dimension; and τ_D is the characteristic time of the reaction-limited aggregation.

In contrast, the RLA model suggested that not every contact between two particles in solution results in them sticking to one another (repulsion between the colloidal particles); thus, the particle growth was described by slow-aggregation kinetics, as in eq 2:

$$R = R_o\exp\left[\frac{t}{\tau_R d_f}\right] \quad (2)$$

where τ_R is the characteristic time of the reaction-limited aggregation.

Genetic algorithm (GA) codes using particle swarm optimization were employed in MATLAB to generate the adjustable parameters for the employed models, which were fractal dimension (d_f), reaction time (τ_d), and diffusion time (τ_r).

3. RESULTS AND DISCUSSION

The effects of long time on the key factors affecting asphaltene precipitations were critically evaluated. The literature highlighted the significant effects of asphaltene precipitation when studied upon longer contact times (from days to months).[15] For example, the effects of temperature on the precipitation of asphaltenes were contradicting in the literature. Maqbool et al.[19] highlighted that increasing temperature increased asphaltene solubility in the crude oil system, thus resulting in fewer asphaltene precipitations. Their work was however limited to 50 °C. Ghanavati et al.[20] hinted that upon increasing temperature (25−85 °C), the solubility of resins increased and the viscosity of the crude system reduced. A system of such nature promoted increasing asphaltene precipitations. However, the effect of time was not considered.

To clarify the doubts on the effects of key factors (such as temperature) affecting asphaltene precipitations, the consideration of room and reservoir conditions in a long kinetic time is needed to ensure that the crude oil system under study reaches its thermodynamic limit. At this point, no further increase in asphaltene precipitations was observed; thus, informed decisions could be made.

3.1. Effects of Heptol Fraction on Asphaltene Time-Yield Measurements. Filtration experiments were carried out to monitor the effects of composition on asphaltene precipitation for long-time kinetics under harsh experimental conditions. Heptane was used as the precipitant of asphaltenes in the model oil. Varying portions of the precipitant (60 and 50 wt %) were introduced into the prepared model oil mixture. The precipitating asphaltenes were monitored and weighed for varying times (0−7200 min). The effect of heptane concentration significantly impacted the precipitation of asphaltenes. An increase of the precipitant from 50 to 60 wt % in the model oil was observed to induce more precipitation of asphaltenes.

Plotted graphs of the time-dependent yield measurements were obtained from the filtration process at a constant rotation

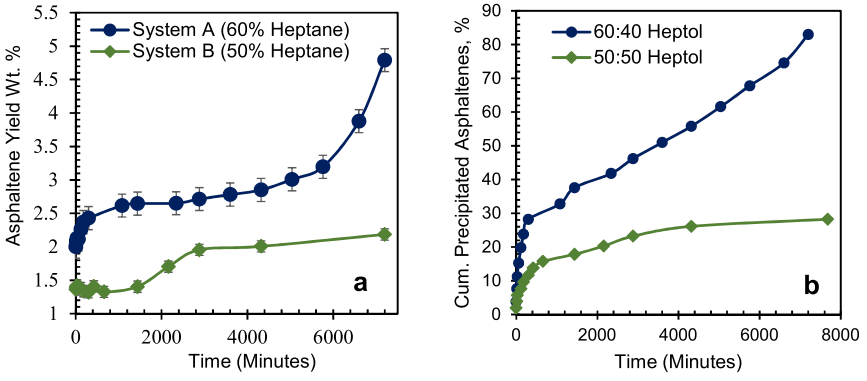

Figure 2. Asphaltene yields (a) and cumulative precipitated asphaltenes (b) at varying studied times for system A (60:40 heptol concentrations) and system B (50:50 heptol concentration).

https://doi.org/10.1021/acs.energyfuels.2c01963
Energy Fuels 2022, 36, 11108−11122

speed (60 rpm), as shown in Figure 2. The researchers observed that the heptol fraction significantly affected the amount of precipitating asphaltenes, including the rate of asphaltene precipitation. Variations of heptol ratios from 1 to 1.5 resulted in an increased yield of asphaltenes. Yudin et al.[31] also confirmed that the presence of heptane concentrations in percentages above the threshold value promoted a dramatic increase in the rate of asphaltene aggregation.

Figure 2b shows that 83% of the total dissolved asphaltenes in the asphaltene−toluene model oil was precipitated within 7200 min for a 60:40 heptol concentration. However, only 27% of the asphaltenes precipitated for a 50:50 heptol concentration. Figure 2a shows the continuous precipitation of asphaltenes upon increasing contact time for the varying heptane concentrations, thus confirming the need for evaluating asphaltene kinetic experimentations at sufficient contact times. The cumulative precipitated asphaltene curves showed that the 50:50 heptol concentration obeyed a power law that indicated only a relatively slow change in the amount of asphaltenes as time increased with an initial amount of 1.89 wt % and an average rate of precipitation at 0.3. Although system B contained a precipitant (heptane), it suggested that the solvent (toluene) employed for preparing the model oil often acted as a barrier limiting the yield of asphaltene precipitation unless neutralized by a higher amount of a precipitant. In contrast, system A with a 1.5:1 ratio of heptol displayed an almost fully linear curve, indicating a significant increase in yield at varying times in the presence of a high precipitant-solvent ratio. Pictures of the filter cakes obtained for each of the studied experiments including the number of systems studied, the time studied (in minutes), and the asphaltene yield percent are presented in Figure 3.

Figure 3A shows the crude oil−heptol system containing 60% heptane, and Figure 3B shows the model oil−heptol system containing 50% heptane. Both figures show a clear distinction in the effect of higher heptane concentrations in the model oil systems. More asphaltenes precipitated for the 60% heptol system as clearly shown in all the pictures in Figure 3A (1−17), whereas the 50% heptol system did not present visible precipitation of asphaltenes in Figure 3B (1−13). However, the varying mass of the filter paper before and after the filtration process suggested the formation of asphaltenes in the 50% heptol model oil system.

3.2. Effects of Rotation Speed on Time-Yield Measurements for System A Model Oil. The effect of rotation speed on the precipitation of asphaltenes was monitored with time. This work employed low and high rotational speeds mimicking low and high production rotational speeds at the pipelines where asphaltenes are mostly deposited during crude oil production. Figure 4a shows the precipitation of asphaltenes under low and high rotational speeds (60 and 150 rpm) for over 7200 min. Under low rotating speed (60 rpm), the asphaltenic model oil displayed varying yield precipitation mechanisms. Both power law and exponential curves indicated that fast and slow aggregation mechanisms were observed throughout the entire studied time. Also, 42% of the asphaltenes dissolved were precipitated from 0 to 2340 min, indicating a power law model (fast kinetics) before slowing down through an exponential model from 2880 to 5760 min. Only a 22% increase in asphaltene precipitation was observed. As the time progressed beyond 5760 min to 7200 min, the trend then changed to a power law model (See Figure 4a,b).

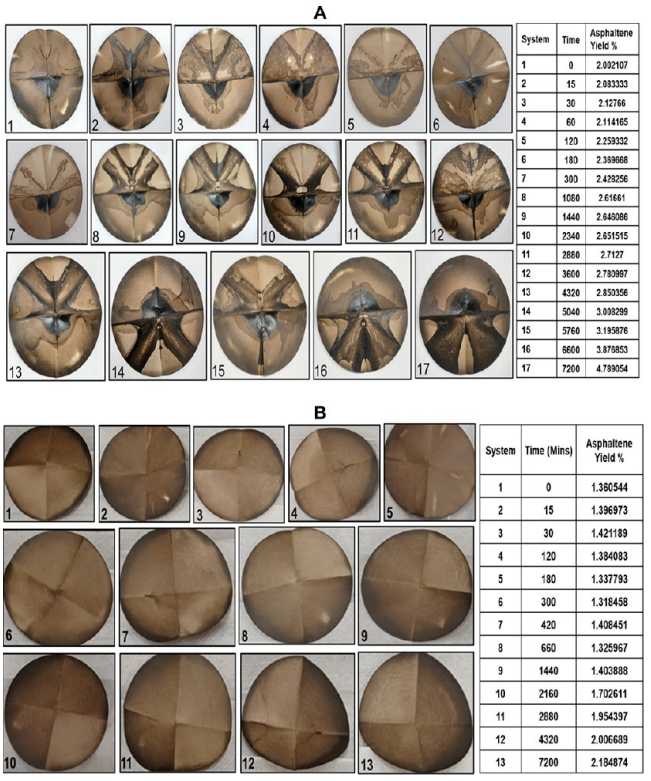

System	Time	Asphaltene Yield %
1	0	2.002107
2	15	2.083333
3	30	2.12766
4	60	2.114165
5	120	2.259332
6	180	2.389668
7	300	2.429256
8	1080	2.61661
9	1440	2.640086
10	2340	2.651515
11	2880	2.7127
12	3600	2.780997
13	4320	2.850356
14	5040	3.008299
15	5760	3.195876
16	6600	3.878853
17	7200	4.789054

System	Time (Mins)	Asphaltene Yield %
1	0	1.360544
2	15	1.396973
3	30	1.421189
4	120	1.384083
5	180	1.337793
6	300	1.318458
7	420	1.408451
8	660	1.325967
9	1440	1.403888
10	2160	1.702611
11	2880	1.954397
12	4320	2.006689
13	7200	2.184874

Figure 3. Filter cakes of precipitated asphaltenes (A) 2.7 μm paper size for 0−7200 min at 60% heptane concentration and (B) 2.7 μm paper size for 0−7200 min at 50% heptane concentration.

A similar precipitation mechanism was also observed in the high rotating fluid at 150 rpm (see Figure 4a @ 150 rpm). These observations were only made from 0 to 2880 min. However, the high rotating fluid displayed induced asphaltene reversibility after 3600 min. After 3600 min, the yield of asphaltenes decreased by 50% (see Figure 4a from 3600 to 4320 min). The decreasing yield of asphaltenes fluctuated between 29 and 52% for the remaining studied time, implying that high rotation speeds induce asphaltene precipitation reversibility, thus causing the disaggregation of asphaltenes in solution leading to their solubility. Increasing rotation speeds, therefore, enhanced asphaltene solubility leading to reduced precipitations. The same observations were made in the works of Rastegari et al.[26] who highlighted the impacts of rotational speed on asphaltene model oil systems. They observed that the precipitation of asphaltene was highly sensitive, and that asphaltene precipitation could be reversed at a high rotational speed. However, they did not consider the effect of contact time on the high rotating fluid, thus limiting the prediction of the starting time of asphaltene reversibility.

This study was conducted for long times, and the high rotating fluid displayed asphaltene reversibility after 3600 min (see Figure 4a). This implied that high rotation speed permitted slow asphaltene precipitation, and upon increasing contact times, it induced the reversibility of the precipitated asphaltenes in the model oil through breakage and enhanced solubility.[26] The rotation speed seemed to destabilize the clusters of precipitating asphaltenes reducing the particle sizes of some formed clusters present in the model oil. However, with increasing contact time, the reversibility of asphaltene ceased and a continuous irreversible trend was observed. Figure 5 shows the impact of high rotation on a model oil

https://doi.org/10.1021/acs.energyfuels.2c01963
Energy Fuels 2022, 36, 11108−11122

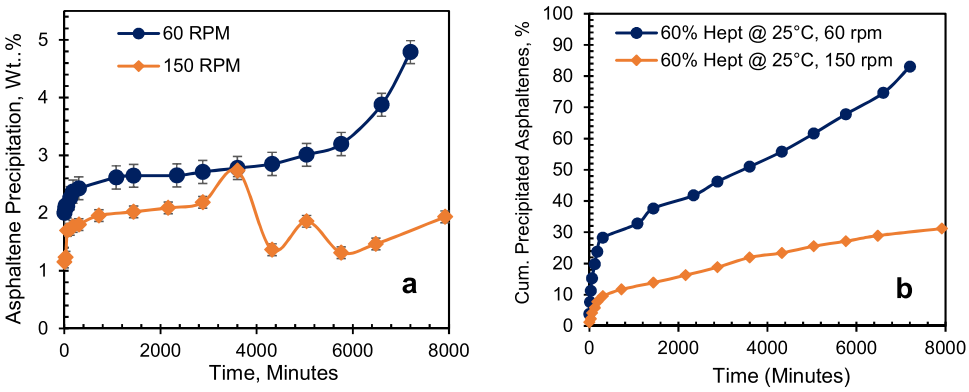

Figure 4. Asphaltene precipitation upon varying rotation speed for system A model oil: (a) asphaltene yield weight % vs time and (b) accumulated asphaltene precipitations vs time.

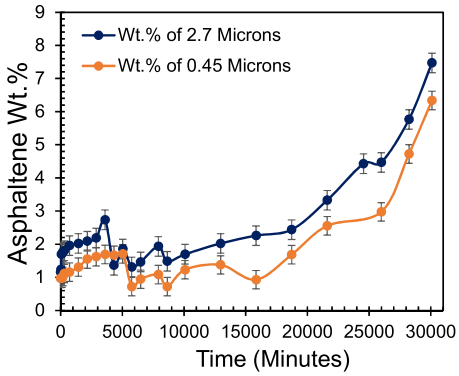

Figure 5. Varying trends of asphaltene precipitation upon high rotation speed (150 rpm) for system A model oil studied for 30,090 min (21 days).

system observed for 21 days (30,090 min) in the presence of varying filter paper sizes. This suggested that asphaltene precipitation in the presence of high rotation would follow an irreversible−reversible−irreversible trend.

3.3. Effects of Varying Pore Sizes on Asphaltene Precipitation. Fakher et al.[14] and Wang et al.[32] highlighted that reservoir properties like pore size contributed to the destabilization of asphaltenes in a given crude system. Following their works, the amount of precipitation was expected to increase as the filter paper was reduced. This is because the small filter paper size was expected to trap more flocculated asphaltenes (even the smaller ones) than the larger sized filter paper.

This study investigated the impact of varying filter paper sizes on the rate of asphaltene precipitation; thus, varying volumes of our model oil on the varying filter paper sizes were employed: 1 mL for the 0.45 μm paper and 1.5 mL on the 2.7 μm paper. The 0.45 μm paper represented the minimum flocculating size for the onset of asphaltene precipitation[33] and 2.7 μm paper for larger flocs of asphaltenes. Both systems were conducted at a rotation speed of 150 rpm and studied for 30,090 min. Figure 6A,B shows the filter cakes obtained after the experimentation for both the 0.45 and 2.7 μm filter paper systems, respectively. The studied time, the number of filtrations carried out, and the associated asphaltene yields corresponding to the studied time for the various systems studied are also illustrated in Figure 6.

Following the slopes of the graph (see Figure 7b), the studied filter papers did not significantly affect the rate of asphaltene precipitation (similar trends were observed). This was observed from the rates of asphaltene precipitation (calculated from the slope of the yield versus time curve) observed in both systems (0.0019 for the 2.7 μm paper and 0.0016 for the 0.45 μm paper). Both systems displayed similar trends indicating similar rates of asphaltene precipitation. The general trend observed for both systems was the initial increase in asphaltene yields followed by a sharp decline (indicating asphaltene reversibility) and then a continuous increase until the end of the studied time. Although the reversibility trends observed in both systems can be attributed to the highly rotated system as discussed earlier in Section 3.2, it was observed that the sharp decline in asphaltene yields occurred earlier in the 2.7 μm filter paper system (after 3600 min). In contrast, the 0.45 μm filter paper system maintained the continuous buildup of asphaltenes until 5040 min (indicating longer asphaltene irreversibility). It can therefore be implied that reservoirs with smaller pore sizes are more likely to delay the reversibility of asphaltenes (see Figure 7a). Furthermore, the filter paper systems studied suggested that pore size does not significantly influence the rate of asphaltene precipitation and flocculation.

The observed increments in asphaltene yields observed in Figure 7a were not because the studied filter papers significantly influenced the rate of asphaltene precipitation but because of the varying amounts of the model oil filtered in the various filter papers. The general difference observed in the yields of both systems (higher yields in 2.7 and lower yields in 0.45 − see Figure 7a) arose from the varying amounts of the model oil utilized in both systems (1 mL of the model oil filtered in the 0.45 μm paper and 1.5 mL filtered in the 2.7 μm paper).

3.4. Effects of Temperature on Asphaltene Yield Measurements for System A Model Oil. The effect of temperature on asphaltene precipitation was also evaluated. The temperature was varied at 25, 50, and 70 °C mimicking room and reservoir conditions. Asphaltene precipitation, as shown in Figure 8, was strongly affected by temperature. More asphaltenes in the model oil solution precipitated at room temperature. 83% of the total dissolved asphaltenes precipitated out of the solution at room temperature, whereas 30% and 38% precipitations of asphaltenes were observed at 50 and 70 °C, respectively. Figure 8A−C shows how temperature affected asphaltene precipitation. A scan of the filtration results confirmed increased solubility of asphaltenes in the model oil as temperature increased from 25−50 °C (see Figure 8B).

https://doi.org/10.1021/acs.energyfuels.2c01963
Energy Fuels 2022, 36, 11108−11122

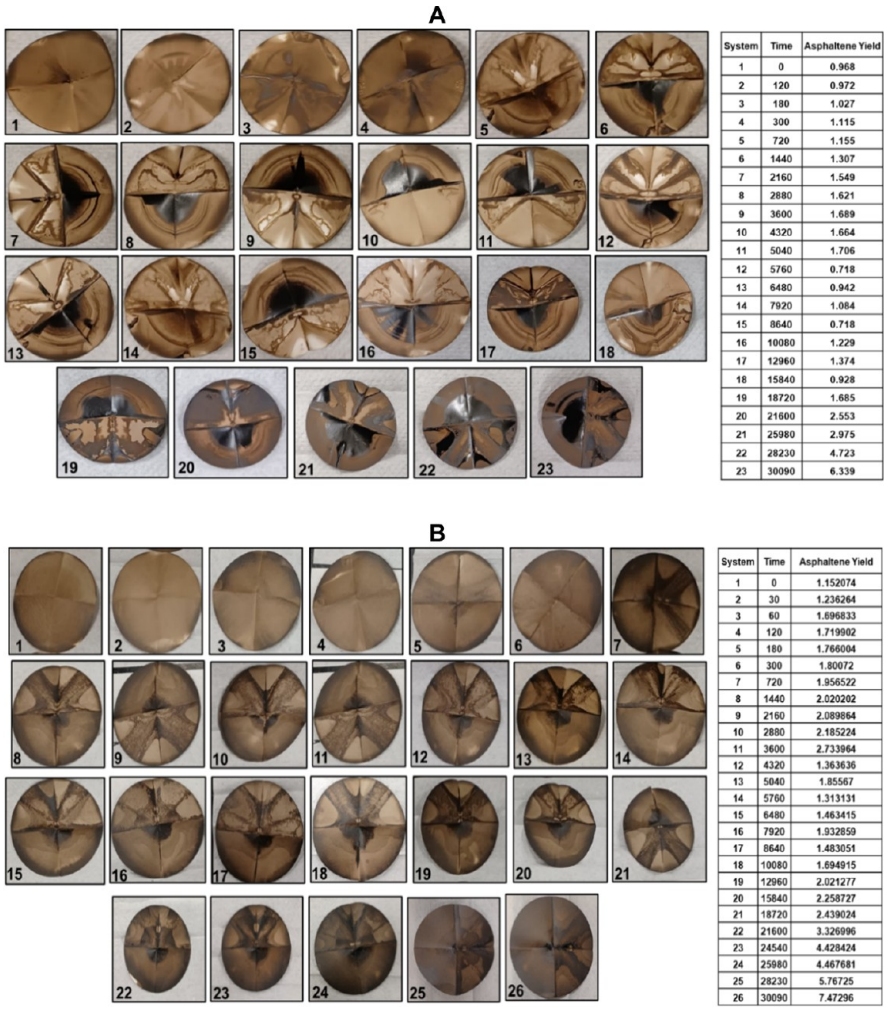

System	Time	Asphaltene Yield
1	0	0.968
2	120	0.972
3	180	1.027
4	300	1.115
5	720	1.155
6	1440	1.307
7	2160	1.549
8	2880	1.621
9	3600	1.689
10	4320	1.664
11	5040	1.706
12	5760	0.718
13	6480	0.942
14	7920	1.084
15	8640	0.718
16	10080	1.229
17	12960	1.374
18	15840	0.928
19	18720	1.685
20	21600	2.553
21	25980	2.975
22	28230	4.723
23	30090	6.339

System	Time	Asphaltene Yield
1	0	1.152074
2	30	1.236264
3	60	1.696833
4	120	1.719902
5	180	1.766004
6	300	1.80072
7	720	1.956522
8	1440	2.020202
9	2160	2.089864
10	2880	2.185224
11	3600	2.733964
12	4320	1.363636
13	5040	1.85567
14	5760	1.313131
15	6480	1.463415
16	7920	1.932859
17	8640	1.483051
18	10080	1.694915
19	12960	2.021277
20	15840	2.258727
21	18720	2.439024
22	21600	3.326996
23	24540	4.428424
24	25980	4.467681
25	28230	5.76725
26	30090	7.47296

Figure 6. Filter cakes of precipitated asphaltenes (A) 0.45 μm paper size for 0−30,090 min at 60% heptane concentration and 150 rpm and (B) 2.7 μm paper size for 0−30,090 min at 60% heptane concentration and 150 rpm.

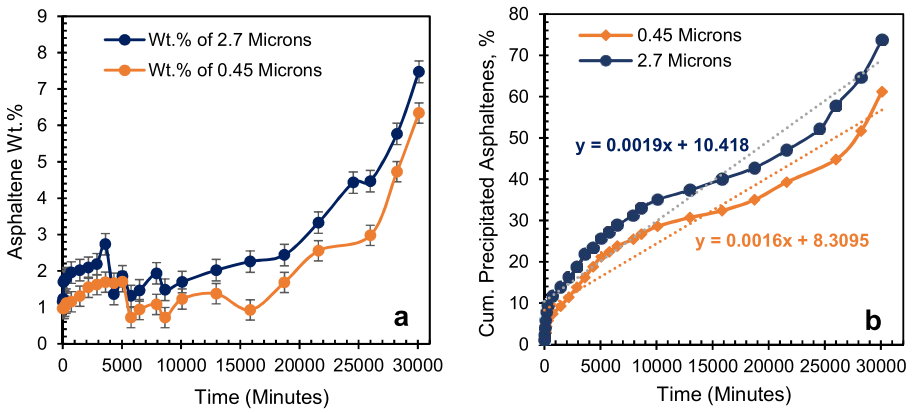

Figure 7. Asphaltene yields (a) and cumulative precipitated asphaltenes for system A model oil (b) at varying studied times collected on both 0.45 and 2.7 μm filter papers at 150 rpm and room temperature conditions. 1 mL of the model oil was filtered in the 0.45 μm paper, and 1.5 mL of the model oil was filtered in the 2.7 μm paper.

No clear asphaltene precipitations were observed for almost 1440 min of contact time (see the first six pictures of Figure 8B). This confirmed low asphaltene precipitation due to enhanced solubility as the temperature of the system was increased from room temperature to 50 °C. Conversely, although the increase in the system's temperature from 50−70 °C generally improved the solubility of asphaltenes (resulting in lower asphaltene precipitations) in the system utilized, a contradicting trend was observed in the early time region (0−60 min).

From Figure 9a, the model oil systems for 50 and 70 °C displayed higher asphaltene yields at the early time regions. The higher asphaltene yields suggested that increasing temperature promoted the fast nucleation of asphaltenes in

https://doi.org/10.1021/acs.energyfuels.2c01963
Energy Fuels 2022, 36, 11108−11122

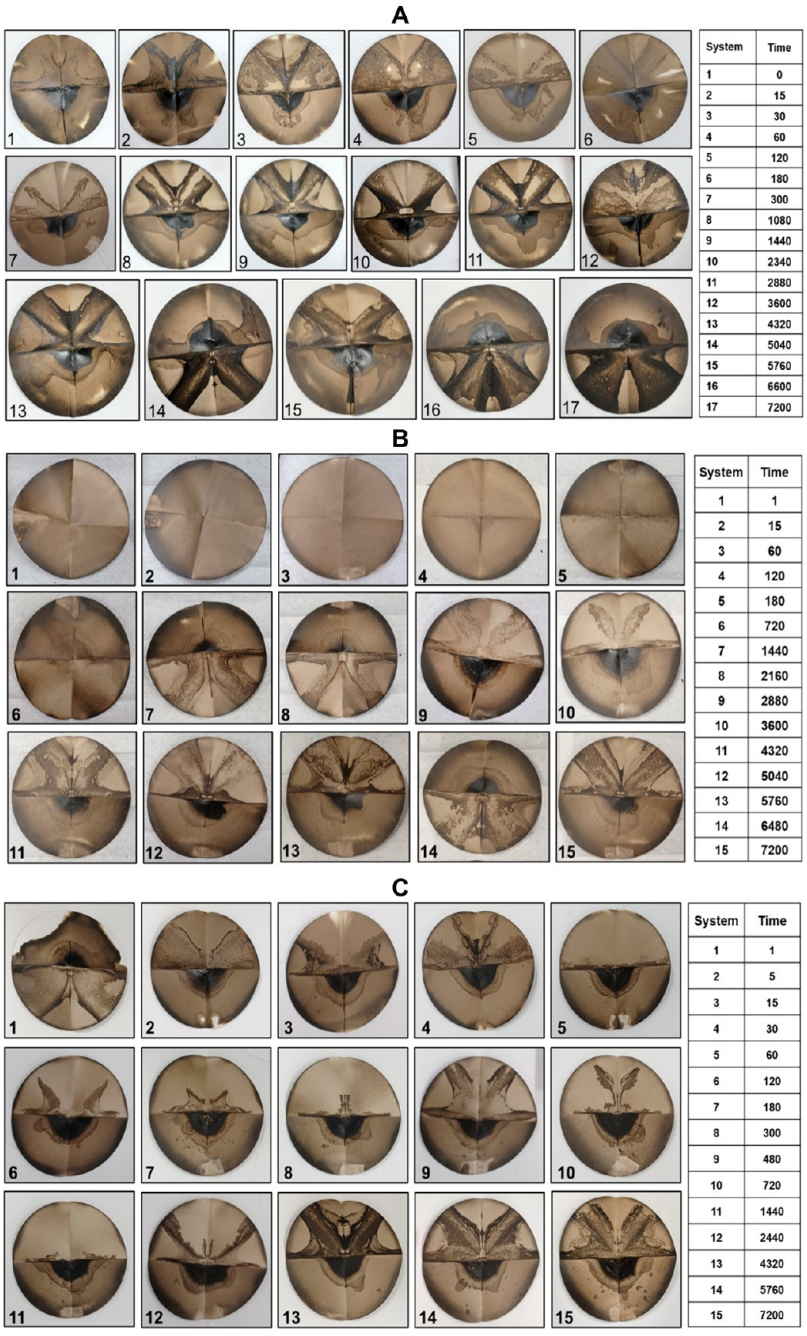

Figure 8. Filter cakes of precipitated asphaltenes: (A) 2.7 μm paper size for 0−7200 min at 25 °C, (B) 2.7 μm paper size for 0−7200 min at 50 °C, and (C) 2.7 μm paper size for 0−7200 min at 70 °C.

the given model oil systems. This fast reaction occurred within the first hour after which a significant reduction in the yield of asphaltenes was observed. The reduction in asphaltene yield after initially showing fast kinetic precipitation suggested a cross-behavior effect of asphaltenes (unstable asphaltenes to soluble asphaltenes) in the model oil system. Thus, the observations of temperature-kinetic experiments were therefore time-dependent. Observations at low contact times presented higher asphaltene precipitations; however, as time progressed, the asphaltenes became soluble in the system, resulting in lower asphaltene precipitations. Thus, conclusions of asphaltene precipitation temperature-kinetic experiments at short time scales are likely to be a misrepresentation of the general trend, hence the need for longer contact time experiments.

Figure 9b shows the plot of the cumulative amount of asphaltenes precipitated at varying times for the studied temperatures. The rate of asphaltene precipitation was reduced almost 3 times as the temperature was increased from 25 to 50 °C. They however followed similar linear trends with R^2 fittings of 94 and 95% respectively. The system under 70 °C observed a power law model, suggesting that upon further studied time, its system would likely reach equilibrium upon which no further increase in asphaltene precipitation would be observed due to enhanced asphaltene solubility in the model system. Therefore, in a thorough comparison of both Figure 9a,b within the studied time frame (7200 min), increased

https://doi.org/10.1021/acs.energyfuels.2c01963
Energy Fuels 2022, 36, 11108−11122

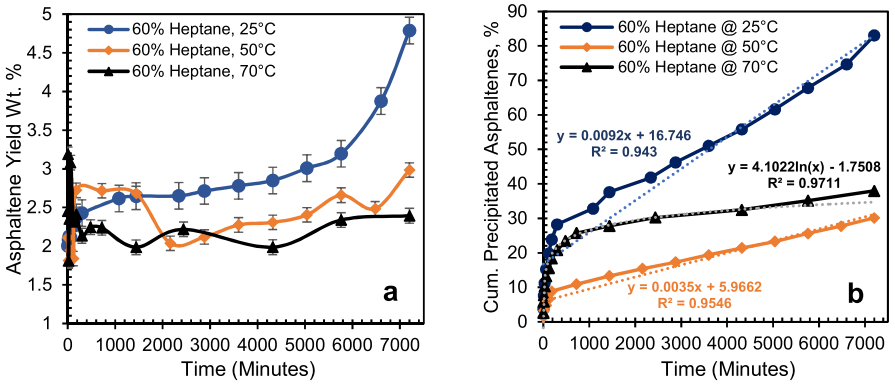

Figure 9. (a) Asphaltene wt % versus time for system A model oil and (b) cumulative precipitating asphaltenes with time for system A model oil.

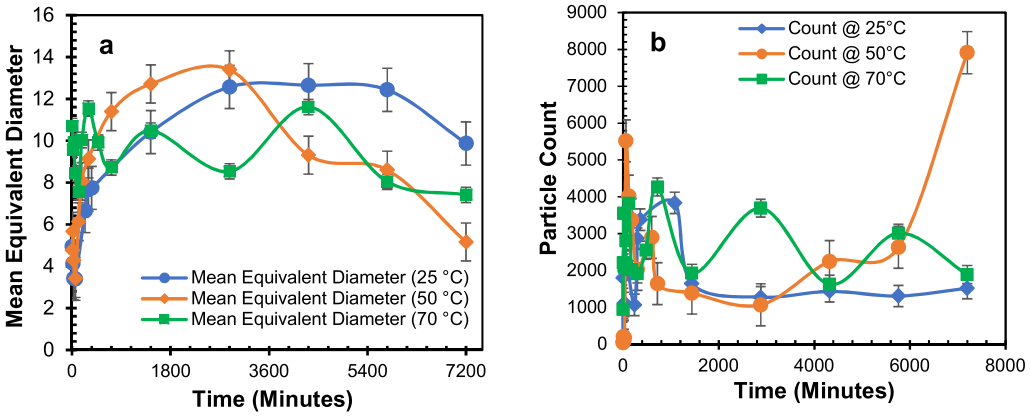

Figure 10. (a) Asphaltene particle size distributions studied at 25, 50, and 70 °C from 0 to 7200 min for system A model oil and (b) particle count distributions observed at 25, 50, and 70 °C from 0 to 120 h for system A model oil.

temperature would significantly reduce asphaltene precipitation until it reached the temperature that promotes fast nucleation and precipitation.[34] More asphaltene precipitations are likely to occur for a new producing well due to the promotion of fast nucleation of asphaltenes at early times. Hence, during such early productions, the introduction of asphaltene precipitation inhibitors was greatly encouraged in systems utilized to improve oil recovery. The use of these inhibitors was bound to decrease sharply as production time continues due to enhanced solubility of asphaltenes upon increasing temperature.

3.5. Effects of Temperature on Particle Size-Time Measurements. In this study, the particle size analysis of asphaltene precipitation was studied via confocal microscopy at times varying from 0 to 7200 min. Figure 10a shows the particle size distributions of the asphaltenes at varying temperatures (25−70 °C). In the early time regions (first 360 min), the mean equivalent diameter (MED) followed the order MED at 25 °C < MED at 50 °C < MED at 70 °C (see Table S1). Maqbool et al.[19] confirmed the larger size of precipitating asphaltenes at 50 °C than at 20 °C for 1440 min. In this study, the researchers investigated the impact of longer contact times beyond 1440 min. Although Figure 10a confirms the fast precipitation of asphaltenes with increasing temperature, a varying trend in asphaltene particle size was observed. At contact times beyond 1440 min unto the studied time of 7200 min, the MED order reversed as follows: MED at 70 °C < MED at 50 °C < MED at 25 °C. The variation in the particle sizes of the precipitating asphaltenes confirmed the temperature-dependent nature of asphaltene precipitation. The observed variations were dependent on the contact time studied; hence, the effect of longer contact time should not be overlooked.

In the early time regions (first 1440 min), MED at 25 °C displayed the lowest trends. This suggested the slow buildup of precipitating asphaltenes in the studied medium. The gradual rise in the particle counts of the precipitating asphaltenes as shown in Figure 10b confirmed the slow buildup. The build-up of asphaltene particle sizes was not interrupted for almost the entire studied time at room temperature. Its growth continued until it reached its maximum size of 12.64 μm at 4320 min before showing slight declines from 4320 to 7200 min. Increasing temperatures (at 50 and 70 °C) showed fast precipitation of asphaltenes in the early time regions in the respective oil systems. This was observed in the sharp rise in particle counts and number density for both temperatures (see Table S1). The model oil system observed under 70 °C showed higher asphaltene precipitation over the model system under 50 °C in the early-time regions (0−300 min). Table S1 shows the particle counts and particle size distributions of the confocal images obtained from the 60% *n*-heptane model oil at varying times from 0 to 7200 min, and varying temperatures were found at 25, 50, and 70 °C.

The obtained results confirmed the impact of increasing temperature on asphaltene size. However, the growth of particle sizes decreased after reaching its peak MED of 11.54 μm for the first 300 min in the 70 °C model oil system. The sharp decrease in the particle size was probably due to the enhancement of asphaltene solubility upon increasing temperature.[17] In contrast, the particle sizes of the 50 °C model oil

https://doi.org/10.1021/acs.energyfuels.2c01963
Energy Fuels 2022, 36, 11108−11122

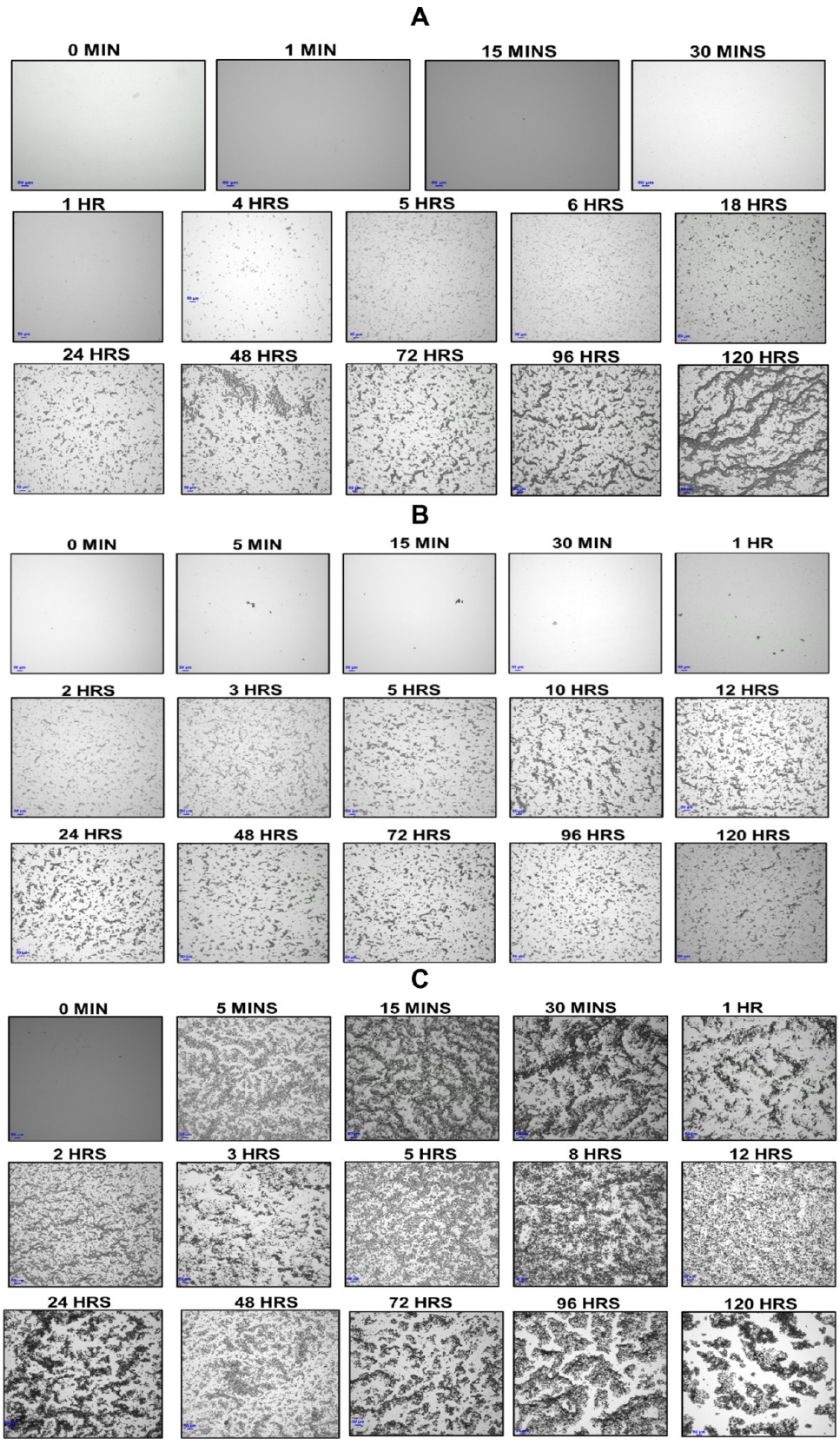

Figure 11. Confocal images of the model oil flocculated with (A) 60% *n*-heptane at varying times from 0 to 7200 min at 25 °C with a scale bar of 50 μm, (B) 60% *n*-heptane at varying times from 0 to 7200 min at 50 °C with a scale bar of 50 μm, and (C) 60% *n*-heptane at varying times from 0 to 7200 min at 70 °C with a scale bar of 50 μm.

system maintained a consistent buildup for 2880 min reaching an MED of 13.39 μm. This suggested that for 0 to 2880 min, a temperature of 50 °C was not sufficient to stimulate the solubility of the asphaltene content of the studied medium.

https://doi.org/10.1021/acs.energyfuels.2c01963
Energy Fuels 2022, 36, 11108−11122

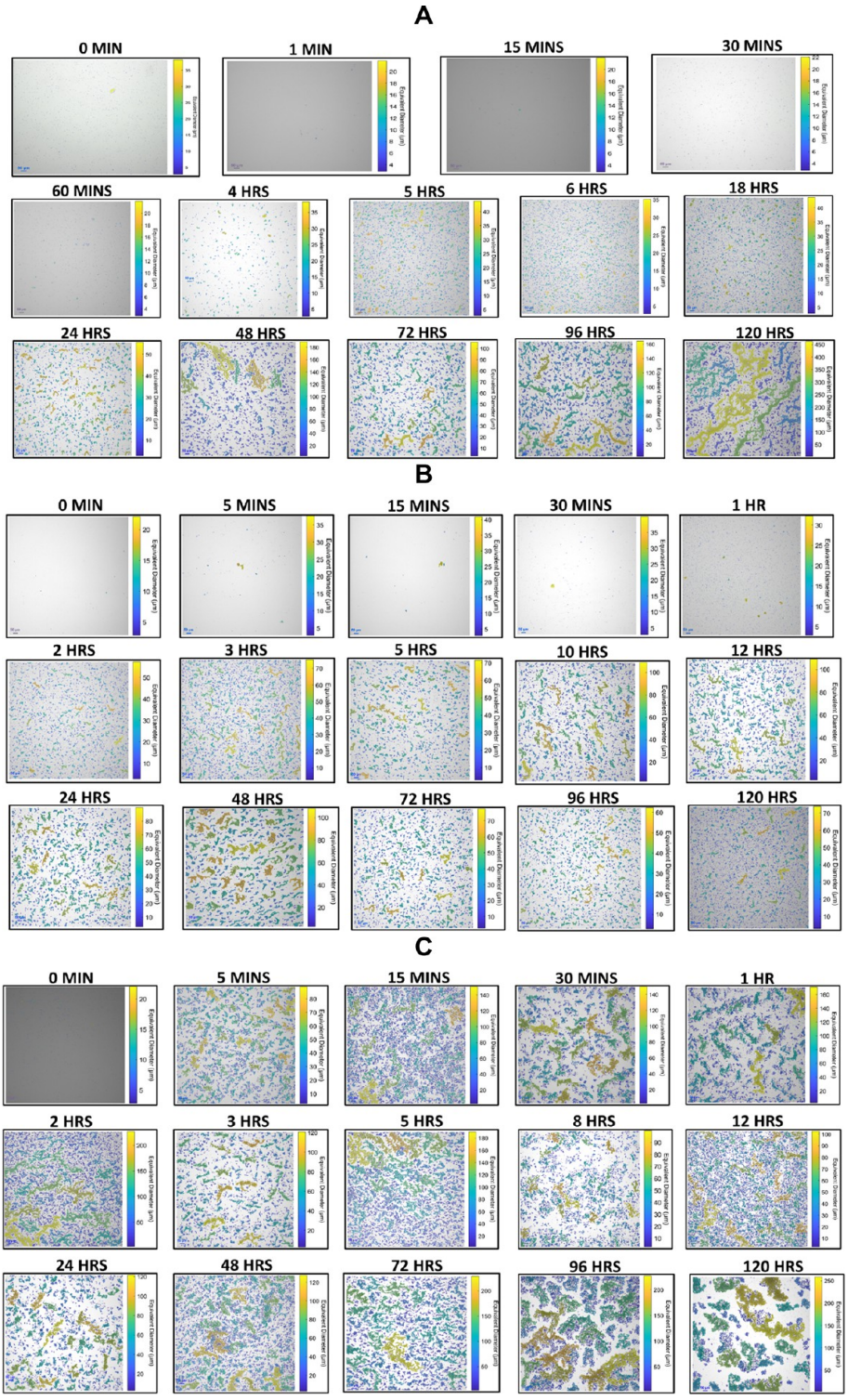

Figure 12. Processed confocal images (A) 60% *n*-heptane at varying times from 0 to 7200 min at 25 °C with a scale bar of 50 μm, (B) 60% *n*-heptane at varying times from 0 to 7200 min at 50 °C with a scale bar of 50 μm, and (C) 60% *n*-heptane at varying times from 0 to 7200 min at 70 °C with a scale bar of 50 μm.

However, after 2880 min, a sharp decline in the MED from 2880 to 7200 min was noticed. The confocal experimentation confirmed the accumulated yield experiments, which implied that asphaltene precipitation yielded more regarding decreasing temperature. Irrespective of the fast rate of asphaltene precipitation upon increasing temperature, the continuous heating of the model oil systems increased the stability of asphaltenes in the model oil system. This was the probable reason for the reversibility observed in asphaltene yields and sizes upon increasing temperatures.

Figures 11 and 12 show the original and processed images obtained from the confocal microscope, respectively. At 25 °C, the confocal images display the slow buildup of precipitating asphaltenes (see Figures 11A and 12A). This continued until

https://doi.org/10.1021/acs.energyfuels.2c01963
Energy Fuels 2022, 36, 11108−11122

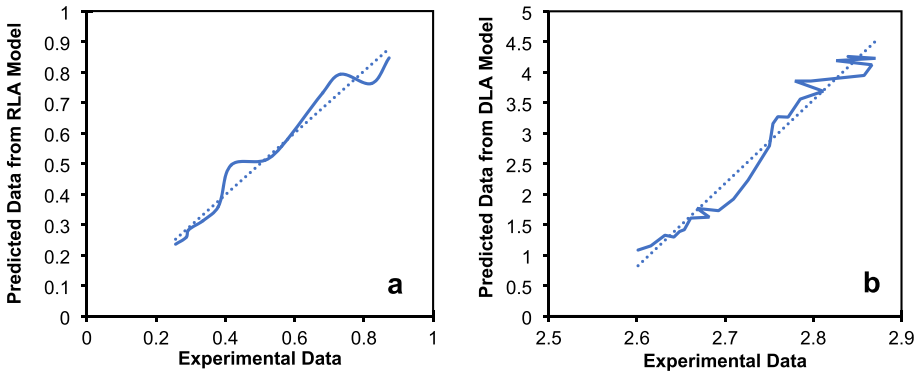

Figure 13. Comparison of asphaltene diametric sizes predicted from (a) the general RLA equation with extracted data and (b) general DLA equation with extracted data. Data was extracted from Yudin et al.[31]

1440 min. However, the system changed at 2880 min and a large build-up of asphaltene precipitating was then observed. At 50 °C, the confocal images displayed early buildup of precipitating asphaltenes from 120 min (see Figures 11B and 12B). This continued until 2880 min, and then a lower particle size was observed. At 70 °C, the confocal images started displaying the early buildup of asphaltene particle size from 5 min (see Figures 11C and 12C). This continued until 1440 min, and then a lower particle size was observed. The reason for the lower particle size was the model oil system approaching a glass transition point upon increasing temperature. At this point, the system transitioned from a precipitating state to a solubility state, hence the wavery nature of the images (see Figure 11C).

3.6. Kinetic Modeling of Asphaltene Precipitation.

Herein, the DLVO models (RLA and DLA) were employed to fit the particle size data obtained via the confocal experimentations. These models proved to effectively predict asphaltene particle size under varying times with a good degree of accuracy.[35] However, the asphaltene precipitation phenomenon must be irreversible; thus, conditions such as varying asphaltene concentrations that significantly affect the irreversibility of asphaltenes precipitation limit the use of the DLA model. This study's experimental data for asphaltene precipitation were collected at varying temperatures (25, 50, and 70 °C), as shown in Figure 10a. It was observed that increasing temperature with long studied times (7200 min) stimulated the reversibility of asphaltenes. This potentially rendered the DLVO models insufficient for predicting asphaltene precipitation trends. With this limitation, this work employed the DLVO models to predict the portions of the data that did not show reversibility. Confocal experimental data performed at 25 and 50 °C were utilized for the DLVO modeling predictions.

3.6.1. Developing DLVO Model. First, literature data from Yudin et al.[31] was extracted and employed for developing the DLVO models' algorithm. The codes were used to predict the experimental data and to generate the adjustable parameters of the DLA and RLA models (d_f, τ_D, τ_R). A correct fitting was observed with R^2 values ranging from 0.95 to 0.97 and mean square errors ranging from 0.0016 to 1.15 for both models. The obtained reaction times and fractal dimensions for the RLA equation were 15.78 min and 12.83, respectively, while the diffusion time and fractal dimension of the DLA equation were 5 min and 4.63, respectively. Figure 13a,b shows the quality of the fit of the predicted data to the experimental data. The extracted data are summarized in Table S2.

3.6.2. Modeling Prediction Results. The developed algorithm was utilized to generate the predicted data from the experimental data. The DLVO models have proven to be good predictors of asphaltene precipitation data under irreversibility reactions, so the data for the various models were fine-tuned to contain only irreversible data. The experimental data followed a power law equation and fitted the DLA model equation but with high values of d_f. A similar trend was observed by Hung et al.[36] The adjustable parameters of the DLA equation, as predicted by the algorithm, are summarized in Table 5.

Table 5. Parameters of the Predicted Data for the DLA Mechanisms[a]

experimental system	R_o (μm)	τ_D (min)	d_f	MAE
mean equivalent diameter obtained at 25 °C	3.39	54.31	16.52	4.44
mean equivalent diameter obtained at 50 °C	3.41	54.47	9.75	5.15

[a]MAE − mean absolute error; R_o − initial radius; τ_D − diffusion time; d_f − fractal dimension.

Figure 14a,b (as shown above) shows graphs of the predicted and experimental data for the varying asphaltene mean equivalent diameter. Furthermore, literature data was extracted from Soulgani et al.[37] who investigated the precipitation of asphaltenes in a similar model oil system comprising toluene, hexane, and asphaltenes. The data, as shown in Figure 15a, followed a power law curve representative of the DLA model. The predicted versus experimental outcomes utilizing the DLA equation are shown in Figure 15b. The obtained diffusion time and fractal dimension for the data were 12.99 min and 2.57, respectively. The mean absolute error obtained was 0.43. Herein, the researchers observed that the DLVO models did not effectively predict the data trend; thus, a more accurate model is required to effectively predict time-particle size asphaltene data.

The DLVO models were incapable of predicting asphaltene precipitations under high temperatures due to the induced reversibility trends imposed on the system. Also, the literature showed other limitations of using DLVO at higher heptol concentrations. Figure 16a,b shows the varying trends in asphaltene particle size incapable of DLVO predictions under higher concentrations and higher temperatures. Alternative

https://doi.org/10.1021/acs.energyfuels.2c01963
Energy Fuels 2022, 36, 11108−11122

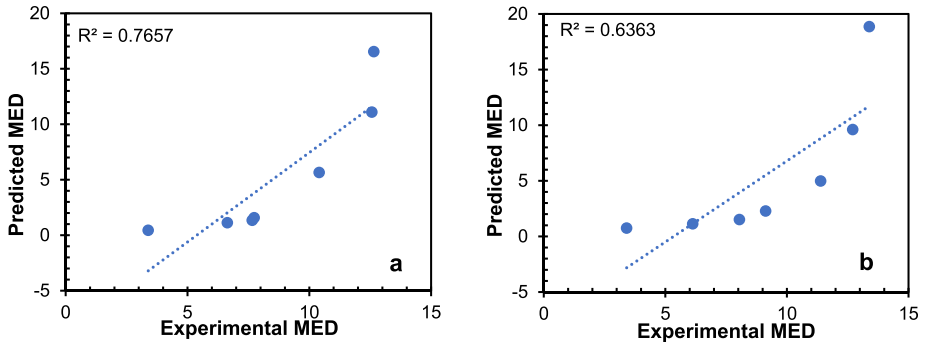

Figure 14. Asphaltene particle sizes predicted from (a) the general DLA equation with experimental data performed at 25 °C and (b) general DLA equation with experimental data performed at 50 °C.

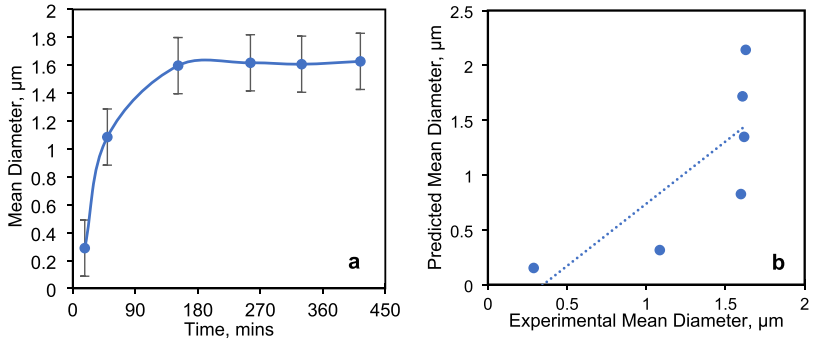

Figure 15. Asphaltene particle size distributions: (a) DLA trends observed with experimental data and (b) predicted vs experimental outcomes utilizing the DLA equation. Data from Soulgani e al.[37]

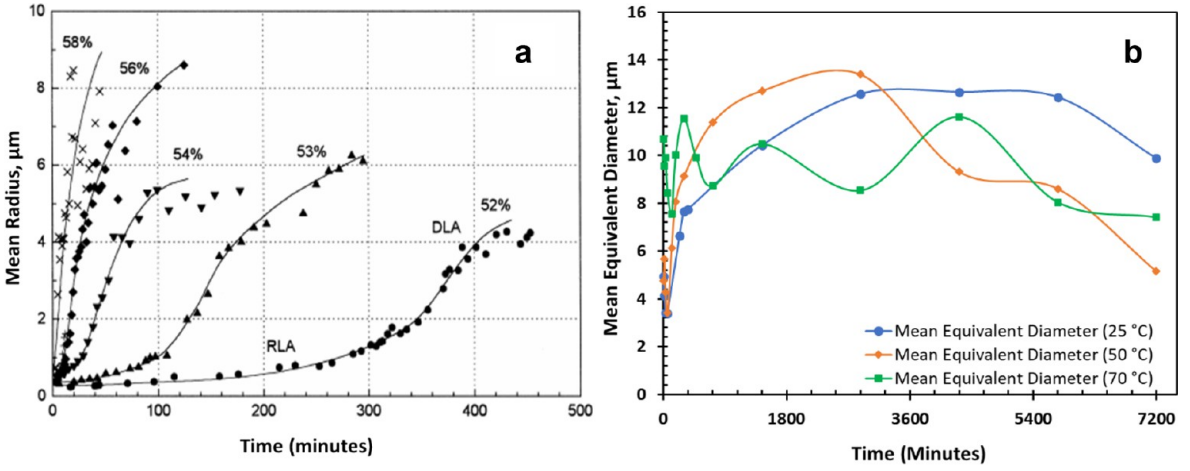

Figure 16. Changing trends of asphaltene particle size distributions at (a) varying heptol concentration effects by Yudin et al.[31] and (b) varying temperature effects from our experimentation.

kinetic models capable of predicting asphaltene precipitations under harsh conditions are thus needed.

4. CONCLUSIONS

This work investigated the effect of long-time kinetics on the thermodynamic parameters influencing asphaltene precipitation. Investigated parameters included the composition of the crude, temperature (room and reservoir conditions), varying rotation speed, and varying pore sizes under an atmospheric pressure condition. The following statements concluded the findings:

a. The effect of time on asphaltene precipitation was dependent on the type of thermodynamic parameter under consideration. For example, it was observed that the effect of heptane concentration and temperature was reproduced at times around 2880 min while an extended amount of time was required for thermodynamic parameters such as rotational speed and pore size. The study of short times below 2880 min was prone to inaccuracies resulting from the initial hysteresis process of asphaltene precipitation.

b. Asphaltene precipitation was significantly affected by the composition of the crude, temperature, and rotation speed as follows: composition > rotation speed > temperature. Thus, a system that avoids significant contact between the CO_2 and the crude during gas

https://doi.org/10.1021/acs.energyfuels.2c01963
Energy Fuels 2022, 36, 11108−11122

flooding, including maintaining a high rotation speed under reservoir temperature, is more likely to exhibit low asphaltene precipitation. The studied pore sizes did not significantly affect asphaltene precipitation.

c. Increasing temperature enhanced asphaltene precipitation in early time regions; thus, more asphaltenes were likely to deposit in the early times of production. This reduced production time due to increased solubility of asphaltenes upon time variations.

d. Increasing temperature enhanced asphaltene solubility and shortened the onset time of asphaltene precipitation. Furthermore, the reversibility of asphaltene precipitation in crude was promoted by increasing the temperature and rotation speed of the medium where the crude was.

e. DLVO modeling asphaltene predictions did not effectively predict the particle size trends of the confocal experimental data, hence the need for new kinetic models capable of predicting varying literature data.

5. RECOMMENDATION

To clarify the effects of pore size on the rate of asphaltene precipitation, more kinetic studies with varying filter paper sizes studied under similar conditions and systems are needed. Furthermore, the cross-behavior pattern of asphaltene precipitation caused by increasing temperatures in the model oil systems requires further study to clarify the exact reason for the behavioral pattern. Also, investigations of asphaltene precipitation and depositions in light oils with suitable asphaltene contents are needed. Next, the incorporation of a wide array of heptol systems signifying varying composition (not only 60 heptol content) is needed for investigating thermodynamic parameters such as temperature, composition, pore size, and rotation speed. This work employed the use of unwashed asphaltenes via the modified IP 143 method for experimentations, and it is thus necessary to investigate the impact of asphaltene type (washed asphaltenes obtained via the standard procedure) on the precipitation and deposition of asphaltenes. Last, studies that involve the use of computational tools like COSMO-RS or COSMO-SAC that employ quantum chemical calculation of molecular structures to predict the thermophysical and chemical properties of solute-solvent reactions like asphaltene solubility in varying solvents are also needed.[38−41]

ASSOCIATED CONTENT

Supporting Information

The Supporting Information is available free of charge at https://pubs.acs.org/doi/10.1021/acs.energyfuels.2c01963.

Actual sizes of the confocal images including their processed images as obtained from the 60% *n*-heptane model oil system for the various studied times and varying temperature studies (PDF)

AUTHOR INFORMATION

Corresponding Author

Abdulmohsin Imqam − *Geosciences and Geological Engineering and Petroleum Engineering Department, Missouri University of Science and Technology, Rolla, Missouri 65401, United States;* orcid.org/0000-0003-1783-7491; Phone: +1(573) 341-4669; Email: aimqam@mst.edu

Author

Ato Kwamena Quainoo − *Geosciences and Geological Engineering and Petroleum Engineering Department, Missouri University of Science and Technology, Rolla, Missouri 65401, United States;* orcid.org/0000-0001-9014-7038

Complete contact information is available at: https://pubs.acs.org/10.1021/acs.energyfuels.2c01963

Notes

The authors declare no competing financial interest.

Ato Kwamena Quainoo: Methodology, Experimentation, Writing - original draft, Writing - review & editing. **Imqam Abdulmohsin**: Conceptualization, Validation, Writing - Review & Editing, Supervision and Funding.

ACKNOWLEDGMENTS

The authors express their deepest gratitude to the US National Science Foundation, Chemical, Biological, Environmental, and Transport Systems for funding this work under the grant CBET-1932965 and to the Missouri University of Science and Technology for providing a suitable working environment for the experimentation.

REFERENCES

(1) Tackie-Otoo, B. N.; Ayoub Mohammed, M. A.; Yekeen, N.; Negash, B. M. Alternative Chemical Agents for Alkalis , Surfactants and Polymers for Enhanced Oil Recovery: Research Trend and Prospects. *J. Pet. Sci. Eng.* **2020**, *187*, 106828.

(2) Elturki, M.; Imqam, A. Asphaltene Thermodynamic Precipitation during Miscible Nitrogen Gas Injection. *SPE J.* **2022**, 877−894.

(3) Buriro, M. A.; Shuker, M. T. Minimizing Asphaltene Precipitation in Malaysian Reservoir. In *SPE Saudi Arabia Section Technical Symposium and Exhibition;* OnePetro: 2013, No. Figure 1, 517−526, DOI: 10.2118/168105-ms.

(4) Fakher, S.; Imqam, A. Asphaltene Precipitation and Deposition during CO2 Injection in Nano Shale Pore Structure and Its Impact on Oil Recovery. *Fuel* **2019**, *237*, 1029−1039.

(5) Alfarge, D.; Wei, M.; Bai, B.; Alsaba, M. Lessons Learned from IOR Pilots in Bakken Formation by Using Numerical Simulation. *J. Pet. Sci. Eng.* **2018**, *171*, 1−15.

(6) Fakher, S.; Imqam, A. Investigating and Mitigating Asphaltene Precipitation and Deposition in Low Permeability Oil Reservoirs during Carbon Dioxide Flooding to Increase Oil Recovery. In *SPE Annual Caspian Technical Conference and Exhibition;* OnePetro: 2018, DOI: 10.2118/192558-MS.

(7) Maqbool, T.; Raha, S.; Hoepfner, M. P.; Fogler, H. S. Modeling the Aggregation of Asphaltene Nanoaggregates in Crude Oil-Precipitant Systems. *Energy Fuels* **2011**, *25*, 1585−1596.

(8) Branco, V. A. M.; Mansoori, G. A.; De Almeida Xavier, L. C.; Park, S. J.; Manafi, H. Asphaltene Flocculation and Collapse from Petroleum Fluids. *J. Pet. Sci. Eng.* **2001**, *32*, 217−230.

(9) Mohammed, I.; Mahmoud, M.; El-Husseiny, A.; Al Shehri, D.; Al-Garadi, K.; Kamal, M. S.; Alade, O. S. Impact of Asphaltene Precipitation and Deposition on Wettability and Permeability. *ACS Omega* **2021**, *6*, 20091−20102.

(10) Buriro, M. A.; Shuker, M. T. Asphaltene Prediction and Prevention: A Strategy to Control Asphaltene Precipitation. In *SPE/PAPG Annual Technical Conference;* OnePetro: 2012, 21−31, DOI: 10.2118/163129-ms.

(11) Fakher, S.; Ahdaya, M.; Elturki, M.; Imqam, A. Critical Review of Asphaltene Properties and Factors Impacting Its Stability in Crude Oil. *J. Pet. Explor. Prod. Technol.* **2020**, *10*, 1183−1200.

(12) Creek, J. L. Freedom of Action in the State of Asphaltenes: Escape from Conventional Wisdom. *Energy Fuels* **2005**, 1212−1224.

(13) Fakher, S.; Ahdaya, M.; Elturki, M.; Imqam, A.; Abdelaal, H. Roadmap to Asphaltene Characteristics, Properties and Presence in Crude Oils Based on an Updated Database from Laboratory Studies. In *Carbon Management Technology Conference;* OnePetro: 2019, DOI: 10.7122/cmtc-558560-ms.
(14) Fakher, S.; Ahdaya, M.; Elturki, M.; Imqam, A. An Experimental Investigation of Asphaltene Stability in Heavy Crude Oil during Carbon Dioxide Injection. *J. Pet. Explor. Prod. Technol.* **2020**, *10*, 919−931.
(15) Maqbool, T.; Balgoa, A. T.; Fogler, H. S. Revisiting Asphaltene Precipitation from Crude Oils: A Case of Neglected Kinetic Effects. *Energy Fuels* **2009**, *23*, 3681−3686.
(16) Alboudwarej, H.; Beck, J.; Svrcek, W. Y.; Yarranton, H. W.; Akbarzadeh, K. Sensitivity of Asphaltene Properties to Separation Techniques. *Energy Fuels* **2002**, *16*, 462−469.
(17) Alves, C. A.; Romero Yanes, J. F.; Feitosa, F. X.; De Sant'Ana, H. B. Effect of Temperature on Asphaltenes Precipitation: Direct and Indirect Analyses and Phase Equilibrium Study. *Energy Fuels* **2019**, *33*, 6921−6928.
(18) Beck, J.; Svrcek, W. Y.; Yarranton, H. W. Hysteresis in Asphaltene Precipitation and Redissolution. *Energy Fuels* **2005**, *19*, 944−947.
(19) Maqbool, T.; Srikiratiwong, P.; Fogler, H. S. Effect of Temperature on the Precipitation Kinetics of Asphaltenes. *Energy Fuels* **2011**, *25*, 694−700.
(20) Ghanavati, M.; Shojaei, M.-J.; Ahmad Ramazani, S. A. Effects of Asphaltene Content and Temperature on Viscosity of Iranian Heavy Crude Oil: Experimental and Modeling Study. *Energy Fuels* **2013**, *27*, 7217−7232.
(21) Ghosh, A. K.; Chaudhuri, P.; Kumar, B.; Panja, S. S. Review on Aggregation of Asphaltene Vis-a-Vis Spectroscopic Studies. *Fuel* **2016**, *185*, 541−554.
(22) Enayat, S.; Rajan Babu, N.; Kuang, J.; Rezaee, S.; Lu, H.; Tavakkoli, M.; Wang, J.; Vargas, F. M. On the Development of Experimental Methods to Determine the Rates of Asphaltene Precipitation , Aggregation , and Deposition. *Fuel* **2020**, *260*, 116250.
(23) Rogel, E.; Moir, M. Effect of Precipitation Time and Solvent Power on Asphaltene Characteristics. *Fuel* **2017**, *208*, 271−280.
(24) Andersen, S. I. Effect of Precipitation Temperature on the Composition of N-Heptance Asphaltenes Part 2. *Fuel Sci.* **1995**, 579−604.
(25) Escobedo, J.; Mansoori, G. A. Viscometric Determination of the Onset of Asphaltene Flocculation: A Novel Method. *SPE Prod. Facil.* **1995**, 115−118.
(26) Rastegari, K.; Svrcek, W. Y.; Yarranton, H. W. Kinetics of Asphaltene Flocculation. *Ind. Eng. Chem. Res.* **2004**, *43*, 6861−6870.
(27) Andersen, S. I.; Birdi, K. S. Influence of Temperature and Solvent on the Precipitation of Asphaltenes. *Fuel Sci. Technol. Int.* **1990**, *8*, 593−615.
(28) Seifried, C. M.; Crawshaw, J.; Boek, E. S. Kinetics of Asphaltene Aggregation in Crude Oil Studied by Confocal Laser-Scanning Microscopy. *Energy Fuels* **2013**, *27*, 1865−1872.
(29) Ashe, T. R.; Roussis, S. G.; Fedora, J. W.; Felsky, G.; Fitzgerald, W. P. Method for Predicting Chemical or Physical Properties of Crude Oils. U.S. Patent No. 5,699,269, Google Patents December 1997.
(30) Lei, Q.; Zhang, F.; Guan, B.; Liu, G.; Li, X.; Zhu, Z. Influence of Shear on Rheology of the Crude Oil Treated by Flow Improver. *Energy Rep.* **2019**, *5*, 1156−1162.
(31) Yudin, I. K.; Nikolaenko, G. L.; Gorodetskii, E. E.; Kosov, V. I.; Melikyan, V. R.; Markhashov, E. L.; Frot, D.; Briolant, Y. Mechanisms of Asphaltene Aggregation in Toluene-Heptane Mixtures. *J. Pet. Sci. Eng.* **1998**, *20*, 297−301.
(32) Wang, C.; Li, T.; Gao, H.; Zhao, J.; Gao, Y. Quantitative Study on the Blockage Degree of Pores Due to Asphaltene Precipitation in Low-Permeability Reservoirs with NMR Technique. *J. Pet. Sci. Eng.* **2018**, *163*, 703−711.
(33) Negahban, S.; Bahamaish, J. N. M.; Joshi, N.; Nighswander, J.; Jamaluddin, A. K. M. An Experimental Study at an Abu Dhabi Reservoir of Asphaltene Precipitation Caused by Gas Injection. *SPE Prod. Facil.* **2005**, *20*, 115−125.
(34) Bjorøy, Ø.; Fotland, P.; Gilje, E.; Høiland, H. Asphaltene Precipitation from Athabasca Bitumen Using an Aromatic Diluent: A Comparison to Standard n-Alkane Liquid Precipitants at Different Temperatures. *Energy Fuels* **2012**, *26*, 2648−2654.
(35) Rad, M. H.; Tavakolian, M.; Najafi, I.; Ghazanfari, M. H.; Taghikhania, V.; Amani, M. Modeling the Kinetics of Asphaltene Flocculation in Toluene-Pentane Systems for the Case of Sonicated Crude Oils. *Sci. Iran.* **2013**, *20*, 611−616.
(36) Hung, J.; Castillo, J.; Reyes, A. Kinetics of Asphaltene Aggregation in Toluene-Heptane Mixtures Studied by Confocal Microscopy. *Energy Fuels* **2005**, *19*, 898−904.
(37) Soulgani, B. S.; Reisi, F.; Norouzi, F. Investigation into Mechanisms and Kinetics of Asphaltene Aggregation in Toluene/n-Hexane Mixtures. *Pet. Sci.* **2020**, *17*, 457−466.
(38) Quainoo, A. K.; Bavoh, C. B.; Duartey, K. O.; Alhassan, D. Clay Swelling Inhibition Mechanism Based on Inhibitor-Water Interaction : A COSMO-RS Molecular Simulation Approach. *Upstream Oil Gas Technol.* **2022**, *9*, 100080.
(39) Quainoo, A. K.; Negash, B. M.; Bavoh, C. B.; Idris, A.; Shahpin, H. B. A.; Yaw, A. D. Inhibition Impact of Amino Acids on Swelling Clays: An Experimental and COSMO-RS Simulation Evaluation. *Energy Fuels* **2020**, 0c02766.
(40) Islam, M. R.; Hao, Y.; Wang, M.; Chen, C. C. Prediction of Asphaltene Precipitation in Organic Solvents via COSMO-SAC. *Energy Fuels* **2017**, *31*, 8985−8996.
(41) Quainoo, A. K.; Negash, B. M.; Bavoh, C. B.; Idris, A. Natural Amino Acids as Potential Swelling and Dispersion Inhibitors for Montmorillonite-Rich Shale Formations. *J. Pet. Sci. Eng.* **2021**, *196*, 107664.